Progress In Electromagnetics Research M, Vol. 32, 95–113, 2013

COMPLEX PERMITTIVITY LOGGING TOOL EXCITED BY TRANSIENT SIGNAL FOR MWD/LWD

Bin Wang, Kang Li*, Fan Min Kong, and Shi Wei Sheng

School of Information Science and Engineering, Shandong University, Jinan, China

Abstract—This paper proposes a new logging while drilling (LWD) method to evaluate rock moisture content and reservoir hydrocarbon saturation. Transient signal with broadband spectrum covering the sensitive range of fluids contained formation was used as excitation signal in the near-bit MWD system. Continuous measurement in the whole spectrum with both fluid type and saturation changes caused differences in frequency distribution of response signals and achieved integrated evaluation of formation hydrocarbon and water saturation. Linear system analysis was optimized by adding oil/water saturation parameters, and analytic calculating results were presented to verify the performance of the proposed transient MWD system. Compared with conventional wireline and LWD tools, the method presented in this paper provided higher resolution and signal intensity.

1. INTRODUCTION

As oil is a non-renewable resource, after drilling for hundreds of years, petroleum exploration has become more and more complicated due to the decline of oil reserves. The detection of oil/water saturation of reservoirs has become important topics because of surplus oil and reserve formation evaluation [1]. Much work has been done by laboratories and research institutes in recent years [2, 3], and almost all of those studies were based on the theory of frequency dispersive resistivity and permittivity of porous rocks [4, 5]. The frequency dependent characteristics of the formation are affected by the distribution of fluids in the pore space of the rock [6, 7].

Although dry rocks' electric properties are frequency independent below radio frequency, the existence of high porosity and moisture can

Received 11 April 2013, Accepted 6 July 2013, Scheduled 29 July 2013

* Corresponding author: Kang Li (kangli@sdu.edu.cn).

lead to polarization which causes mixture permittivity dispersion [8–10]. In the past twenty years, many authors presented induction tools comparing the apparent resistivity achieved at several hundred kHz and 2 MHz for detection of porous formation resistivity dispersion [11, 12]. But unfortunately, other factors such as invasion, dielectric effects and different antenna structures were found to explain these differences more suitably than resistivity dispersion [13]. Both laboratory research and analysis of practical data showed that electrical permittivity dispersion could be much more apparent if the working frequency range was relatively high. Consequently, parallel instruments as propagation tools with multiple spacing and multiple frequencies have been developed. Dozens of apparent permittivities and conductivities distributed from 20 kHz to 1 GHz can be obtained by the propagation tools [14]. This method can effectively obtain permittivity dispersion and provides a more accurate measurement of the near-borehole region in oil reservoirs, but the accuracy and information integrity obtained from logging data are still limited because of the discrete frequency points. Furthermore, multispacing and multifrequencies structures are practically affected by the differences in vertical resolution and invasion effect, which can possibly cause deviation in multiple detections.

A transient signal is a short-lived signal in a system excited by sudden current shock. Because of the properties belonging to transient signals such as ultra-broad spectrum, elimination of previous influence, and relatively high strength [15], the transient method is widely applied in geophysical prospecting. Ultra-broad electromagnetic well logs were made possible as a new technology twenty years ago [16]. Transient signals are used in this method as transient pulses in both MWD/LWD and wireline logging. The reflected pulses of transient signals caused by adjacent boundaries are used for reservoir navigation and geosteering [17–21]. Various pulse forms of the nanosecond order are used such as instantaneous shut-off signal and transient Gaussian, but broad spectrum and rich information content of the transient signals have not been taken advantage of.

In this paper, a broadband transient pulse excited complex permittivity LWD system for reservoir water/oil saturation and rock matrix texture evaluation is proposed. First, the theory of complex permittivity of moisture formations and practical empirical formulas are introduced. Through analysis of existing laboratory data and logging records, the electrical property spectrum of formations was achieved. Then the structure and operating principle of the LWD system, excited by transient pulse with working frequency span which covers megahertz to gigahertz, are presented in the next

part. This study proposes a linear system analysis combined with oil/water saturation for studying transient pulses propagating through formations with different oil/water saturations. Furthermore, results obtained are discussed and compared to support the new LWD tool.

2. COMPLEX PERMITTIVITY DISPERSION

Reservoir rocks' electrical properties dispersion is the theoretical basis of complex permittivity logging tools, and complex permittivity quantifies the sensitivity of a formation to an alternating electric field excitation. In the frequency range from dozens of megahertz to several gigahertz, three main polarization phenomena contribute to the dielectric dispersive behavior of oil bearing reservoirs: the electronic polarization (rock's inherent permittivity), the molecular polarization (brine water molecules) and the interfacial polarization which is also called Maxwell-Wagner polarization. The three phenomena are determined by different inertial moments of particles, frictions and electrostatics, and each type of polarization will vanish if external electric field exceeds its specific relaxation frequency [22].

All these effects can be described as a polarization density vector $\mathbf{P}$. Plugging this item into Maxwell's equations, effective current through the porous rocks contains two parts: displacement current and conduction current. Maxwell's equations in time domain are [6]:

$$\nabla \times \mathbf{H}(t) = \frac{\partial}{\partial t}\left[\varepsilon_0 \mathbf{E}(t) + \mathbf{P}\right] + \mathbf{J}(t) \tag{1}$$

$$\nabla \times \mathbf{E}(t) = -\frac{\partial \mathbf{B}(t)}{\partial t} = -\mu \frac{\partial \mathbf{H}(t)}{\partial t} \tag{2}$$

In the time harmonic region, by replacing time derivative with $-i\omega$ (ω is the circular frequency) in Equation (1) and Equation (2), Maxwell's equations in frequency domain can be obtained. By solving these equations with elimination method, for homogeneous and isotropic media, the wave number of an electric field can be written as [22]:

$$\mathbf{k} = \frac{\omega}{c}\sqrt{\mu_r}\sqrt{\varepsilon_r + i\frac{\sigma}{\omega\varepsilon_0}} = \frac{\omega}{c}\sqrt{\mu_r}\sqrt{\varepsilon^*} \tag{3}$$

Then the definition of complex permittivity is illustrated from the previous derivation. Conductivity σ, relative permittivity ε_r and frequency ω contribute to complex permittivity at the same time [23]:

$$\varepsilon^* = \varepsilon_r + i\frac{\sigma}{\omega\varepsilon_0} \tag{4}$$

It is known that dry rock matrix permittivity does not depend on frequency as it only benefits from electronic polarization, so it probably plays an insignificant role in rocks at the earth's surface. The frequency dispersion property of a moist reservoir formation exists due to electromagnetic properties of water in porous rocks [24]. Water molecules will change their direction according to an externally applied electric field as they are polar molecules. In addition, they exhibit an electric dipole due to different centers of gravity for positive and negative charges. In this paper, attention is paid to the dielectric frequency dispersion which is caused by water molecule polarization and Maxwell-Wagner polarization. Water molecules' performance under an external electric field is described by the Debye relaxation model [7, 25]. The Debye model for the complex permittivity is as follow:

$$\begin{aligned} \varepsilon' &= \varepsilon_\infty + \frac{\varepsilon_0 - \varepsilon_\infty}{1 + (2\pi f\tau)^2} \\ \varepsilon'' &= \frac{\varepsilon_0 - \varepsilon_\infty}{1 + (2\pi f\tau)^2} 2\pi f\tau + \frac{\sigma}{2\pi f\varepsilon_r} \end{aligned} \tag{5}$$

ε' and ε'' are the real and imaginary parts of the complex permittivity respectively. ε_∞ is the high frequency limit of the permittivity, ε_0 the static limit of the permittivity, and τ the relaxation time constant.

At frequency from dozens of MHz to several GHz, the electric properties of a moist formation are mostly volumetric with respect to the elements and the propagation constant of the rock, water and other compositions. For this reason, many semiempirical models have been advanced to relate soil moisture and microwave dielectric properties [26–28]. Because the formation composition in different reservoirs is complicated and distinguishing, a universal linear model — generalized refractive mixing dielectric model (GRMDM) is proposed as follows [29]:

$$\sqrt{\varepsilon_{formation}} = \begin{cases} \sqrt{\varepsilon_d} + (\sqrt{\varepsilon_b} - 1)W, & W \le W_t \\ \sqrt{\varepsilon_d} + (\sqrt{\varepsilon_b} - 1)W_t + \left(\sqrt{\varepsilon_f} - 1\right)(W - W_t), & W \ge W_t \end{cases} \tag{6}$$

Soil moisture has biphasic dielectric properties, and water in the formation is divided into two parts: bound water and free water. $\varepsilon_{formation}$, ε_b and ε_f are complex permittivity of the formation, bound water and free water, respectively, while ε_d is the complex permittivity of the dried rock matrix and W_t the maximum bound water fraction. When rock moisture is equal to W_t, the next increment of water behaves as free water. In GRMDM, ε_b and ε_f are extensively described by the Debye model.

3. THE TRANSIENT SIGNAL EXCITED BY MWD TOOL

The conventional logging tool operating at frequency below a few hundred kHz is primarily dominated by conductivity. The working frequency range of the new MWD tool is from tens of MHz to GHz, covering the full span of the complex dielectric dispersion of the Maxwell-Wagner polarization sensitive band. In this frequency range, both conductivity and permittivity become predominant, which can be clearly understood from the mechanism of the rock's complex permittivity.

For this purpose, a transient Gaussian pulse with a spectrum from 20 MHz to 1.5 GHz and a center frequency of 500 MHz was applied as a transmitting signal to guarantee the accuracy and integrity of stratigraphic information. Mounting the new LWD system close to the drill bit effectively avoided the interference of mud invasion and borehole collapse. In this way, real time data for formation evaluations were obtained during drill collar penetration before the drilling mud invaded the fresh formation which maximally increased the sensitivity to the virgin zone. Transceiver antennas were designed to be perfect magnetic dipoles, and for signal emission efficiency, ferrite medium was placed on the drill collar. The transmitter was in the center, and two receivers were symmetrically placed around the center [30]. The two receiving rings operated simultaneously to detect the pulses propagating in two different directions for optimal borehole compensation. The location of apparatus and running scenario are shown in Figure 1.

Sensitivity to the formation was taken into consideration in designing the distance between the transmitting and receiving antennas. For the LWD system with a diameter of 12.6 inch, geometrical factors were calculated [22], and two-dimensional diagrams of the geometric factor of tools with antenna spacing of 10 inch, 20 inch, 30 inch, 40 inch are shown in Figure 2. Obviously, the detection zone is not deep enough in the radiation direction for the distance between antennas of 10 inch and 20 inch. Though the sensitivity zone reaches about 30 inch away from the LWD tool for the spacing is 40 inch, the sensitive range became broader, even exceeded the space between the two coils. Furthermore, the sensitivity became lower, at the same time. Taking both detecting depth and sensitivity into consideration, the two symmetrical receiving coils were designed 30 inch from the transmitting coil to tradeoff between the detecting depth and the focusing capability. It is desirable to put more weight on the virgin region farther from the borehole and eliminate the sensitivity to a presumed invaded zone, while the desired focusing effect can be obtained at the same time.

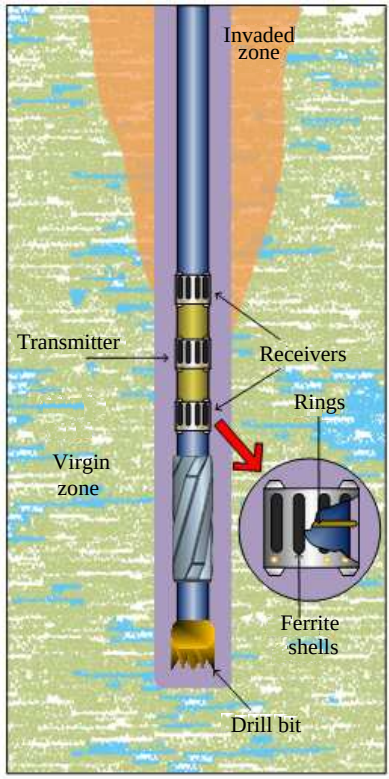

Figure 1. The antenna system of the new LWD tool is mounted near the drill bit, so the detection zone is rarely invaded while the drilling is ongoing and the true propagation properties of the virgin zone are reflected. Signals transmitted by the ring pass through ferrite shells on the drill collar and then penetrate into the formation.

Transient pulse signals were intermittently transmitted as shown in Figure 3, thus receiving signals could be isolated from the influence of previous pulses and at the same time signal strength could be guaranteed. Firstly, before the coil receives the signal, the eddy current caused by previous excitation pulses has already dissipated. Secondly, the tool stores the energy for a period of time, and then launches a transient pulse whose duration is only several nanoseconds. In this way, the transmitting power is critically bigger than that of the tools using continuous excitation like sinusoidal wave and square wave. After spreading in the polarized formation, the spectrum distribution of the signal changed. The basic measurement was to determine

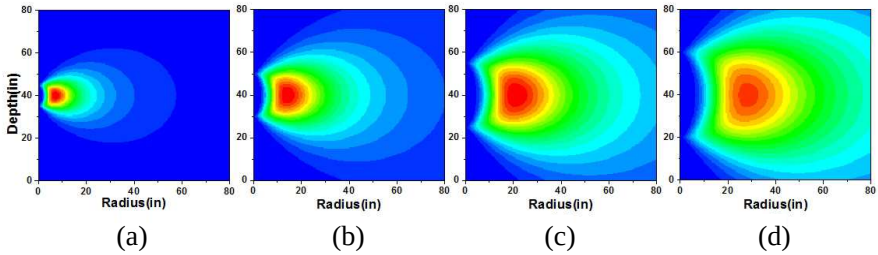

Figure 2. Two-dimensional plot of the geometrical factor of one transmitting and one receiving system with coil distances of (a) 10 in, (b) 20 in, (c) 30 in, (d) 40 in.

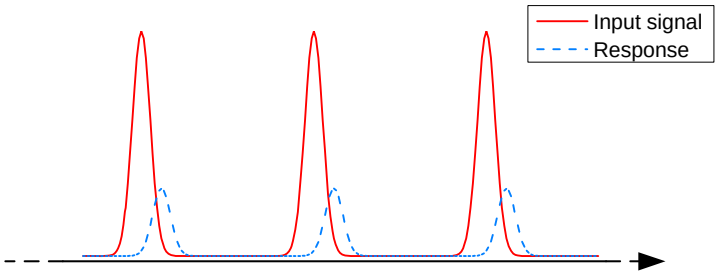

Figure 3. Response signal was isolated from previous transmitting pulses' interference. Energy in downhole environment was precious, and the transient signal saved the limited energy for emitting stronger pulses than continuous signals.

the amplitude attenuation ratio over the whole frequency range. Furthermore, the appropriate band should be chosen according to different sensitive spectrum ranges of the variant formation. Through comparison and processing to amplitude spectrum ratio curves, water and hydrocarbon saturation of virgin zone can be evaluated, and in most cases providing an accurate radial profile of the region close to the borehole. The feasibility and reliability of the new LWD system will be verified in the next section.

4. LINEAR SYSTEM ANALYSIS FOR THE PULSE RESPONSE

Figure 4 shows the essential features of the logging device. It consists of a transmitter ring excited by transient signals and a receiver ring, both of which have the same diameter a. The ring system is presumed to be

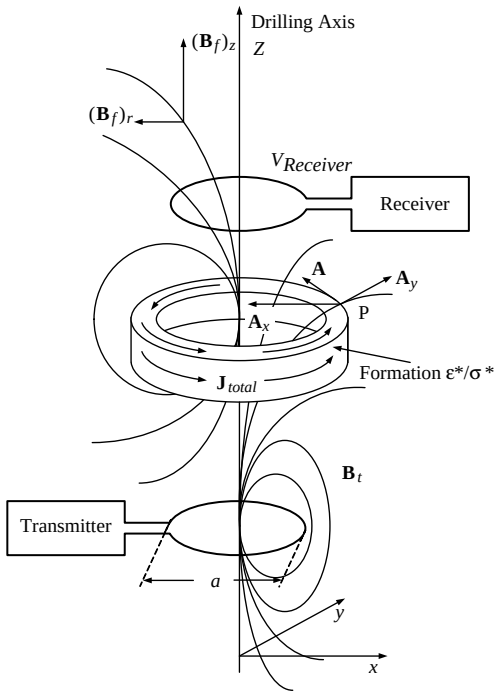

Figure 4. The principle of the tool is theoretically illustrated. The vertical component of the magnetic field produced by the transmitting current induces current in the formation loop. The secondary magnetic field from the formation current brings response voltage to the receiver ring.

surrounded by virgin formation with complex permittivity ε^*, and the formation loop between the two rings is chosen as the representative here.

Magnetic vector potential $\mathbf{A}$ is introduced to describe the vertical component of the magnetic field which is the efficient part affecting the response signal away from the axis of a small current loop (magnetic dipole). The vector potential $\mathbf{A}$ at point P, which is on the formation loop with distance R to the center of transmitter ring, is given by:

$$\mathbf{A} = \frac{\mu p \cos\theta}{4\pi R^2} \tag{7}$$

where p is the dipole moment and θ the angle between the orientation of the dipole and the observation point. For the current loop of the transmitter ring in the x-y plane shown in Figure 4, the expression of $\mathbf{A}$ consists of only two components — $\mathbf{A}_x$ and $\mathbf{A}_y$, since there is no

current distribution in the z direction (direction of the drilling axis). There is nothing influencing the y-component of $\mathbf{A}$ but the y-direction of current of the current loop. By analogy with two charge rods with length equal to the diameter of the loop, the dipole moment will equal $I_0a^2e^{-i\omega t+ikR}$. The exponential term e^{ikR} exists in the imaginary part of the expression of the vector potential, thus it only has influence on the phase information of the final results. While the complex permittivity properties are obtained from the amplitude spectrum, and these approaches take no account of the phase information. In this case, for simplification, the exponential term e^{ikR} is omitted in the following derivation. The cosine of the angle between point P and the dipole is x/R, and then the x-component of the vector potential $\mathbf{A}_y$ can be given by:

$$\mathbf{A}_y = \frac{I_0a^2e^{-i\omega t}\mu x}{4\pi R^3} \tag{8}$$

$\mathbf{A}_x$ can be found by the same method. In this way, the vertical component of the magnetic field of transmitting signal $(\mathbf{B}_t)_z$ at point P can be determined as:

$$\begin{aligned}(\mathbf{B}_t)_z &= (\nabla \times \mathrm{A})_z = \frac{\partial \mathrm{A}_y}{\partial x} - \frac{\partial \mathrm{A}_x}{\partial y} \\ &= \frac{\partial}{\partial x}\left(\frac{I_0e^{-i\omega t}a^2\mu x}{4\pi R^3}\right) + \frac{\partial}{\partial y}\left(\frac{I_0e^{-i\omega t}a^2\mu y}{4\pi R^3}\right) \\ &\propto \frac{I_0e^{-i\omega t}a^2\mu}{4\pi}\left(\frac{1}{R^3} - \frac{3z^2}{R^5}\right)\end{aligned} \tag{9}$$

To simplify the calculation, a harmonic signal substitutes for the broadband signal in the above formula. According to Faraday's law, the electric field $\mathbf{E}$ in the formation loop is established:

$$\nabla \times \mathbf{E} = -\frac{\partial(\mathbf{B}_t)_z}{\partial t} \propto i\omega\frac{I_0e^{-i\omega t}a^2\mu}{4\pi}\left(\frac{1}{R^3} - \frac{3z^2}{R^5}\right) \tag{10}$$

The electric field $\mathbf{E}$, which curl around the z axis, induces a current density $\mathbf{J}_{total}$ in the formation loop, which also behaves as the transmitter ring and sets up its own magnetic field $\mathbf{B}_f$:

$$(\mathbf{B}_f)_z \propto \mathbf{J}_{total} = \sigma^*\mathbf{E} \propto i\omega\frac{I_0e^{-i\omega t}a^2\mu}{4\pi}\left(\frac{1}{R^3} - \frac{3z^2}{R^5}\right)\sigma^* \tag{11}$$

It is proportional to the formation complex conductivity σ^* which has the same physical significance as the complex permittivity ε^* introduced in Part 2. They both show that the total current density

is composed of an induction current and displacement current [31]. So Equation (1) can so be written as:

$$\begin{aligned}\nabla \times \mathbf{H}(\omega) &= -i\omega\varepsilon_0 \left(\varepsilon_r + i\frac{\sigma}{\omega\varepsilon_0}\right)\mathbf{E} = -i\omega\varepsilon_0\varepsilon^*\mathbf{E} \\ &= (\sigma - i\omega\varepsilon_0\varepsilon_r)\,\mathbf{E} = \sigma^*\mathbf{E} = \mathbf{J}_{total} \end{aligned} \tag{12}$$

The vertical component of the secondary magnetic field $(\mathbf{B}_f)_z$ induces a voltage $V_{Receiver}$ at the receiver ring as the response signal.

$$V_{Receiver} \propto -\frac{\partial(\mathbf{B}_f)_z}{\partial t} \propto i\omega^2 \frac{I_0 e^{-i\omega t} a^2 \mu}{4\pi}\left(\frac{1}{R^3} - \frac{3z^2}{R^5}\right)\sigma^* \tag{13}$$

The final result indicates that the voltage detected at the receiver ring directly varies with σ^*/ε^* of the formation. The total current density $\mathbf{J}_{total}$ in the formation loop is strictly proportional to the complex permittivity of tested formation ε^*, and the response signals are directly determined by $\mathbf{J}_{total}$. From a derivation above, the conclusion is drawn that $\mathbf{J}_{total}$ can completely characterize the response signals $V_{Receiver}$ of receiving ring. For a similar distance between rings and excitation signal, the only variable that affects the receiving response is ε^*/σ^*, which forms an important relationship to link the response and frequency dispersive properties of the formation.

In this paper, a method combining linear system analysis with rock oil/water saturation is proposed. As shown in Section 2, frequency dispersive ε and σ determine the electrical properties of rocks. This paper considers a material having conductivity and permittivity which vary with frequency as a linear system, because the reservoir rock is isotropic and time invariant [32]. Electrical parameters of the system presented here are affected by water/oil saturation, complex permittivity of fluids and rock texture's electrical properties. Relationship between input pulse $E(t)$ and response $V(t)$ can be established by the linear system and convolution as shown in Equation (14), where $h(t)$ is the linear system describing the rock sample:

$$\begin{aligned} V(t) &\propto \mathbf{J}_{total}(t) \\ &= \mathbf{E}(t) * h\left\{\left[\sqrt{\varepsilon_d} + \left(\sqrt{\varepsilon^*_{water}} - 1\right)W_{water} + \left(\sqrt{\varepsilon^*_{oil}} - 1\right)W_{oil}\right]^2, t\right\} \end{aligned} \tag{14}$$

Transforming this relationship to the frequency domain, the linear system $h(\omega)$ is described as:

$$\begin{aligned} h(\omega) = &\left[\sqrt{\varepsilon_d(\omega)} + \left(\sqrt{\varepsilon *_{water}(\omega)} - 1\right)W_{water}\right. \\ &\left. + \left(\sqrt{\varepsilon^*_{oil}(\omega)} - 1\right)W_{oil}\right]^2 \frac{a^2\mu}{4\pi}\left(\frac{1}{R^3} - \frac{3z^2}{R^5}\right) \end{aligned} \tag{15}$$

At a frequency of the order of 1 GHz and higher, the complex permittivity is mainly sensitive to water/oil volume, whereas at a frequency of 100 MHz or below, interfacial polarization plays a role. Hence, at the frequency range of tool operation, the response is mostly volumetric with respect to the elements. GRMDM is used to describe the complex permittivity of the oil/water saturated formation in Equation (15). A large amount of experimental data about moist formations' complex permittivity had been previously acquired, which were confirmed as coinciding with the GRMDM volumetric functions. As present in Section 2, several kinds of water contained in formation were subjected to the Debye formula [29].

Extracting a single frequency from the spectrum of the transient signal, the harmonic electric field $E_i(t)$ is divided into two parts: the inphase part and quadrature part after propagation through the linear system. The two parts coincide with the induction current and displacement current constituting the total current $\mathbf{J}_{totali}(t)$ according to laboratory results. We have validated that the receiving voltage is proportional to the $\mathbf{J}_{total}$ in the formation, so by summing every $\mathbf{J}_{totali}(t)$ at single frequencies upward, the normalized whole spectrum of response signals were obtained, which is equal to the result from taking the Fourier transform on output response in the time domain. Linear system behavior of a rock sample is shown in Figure 5. The approximation used in this part is based on the linear theory relation between current density in the formation and voltage in the receiving

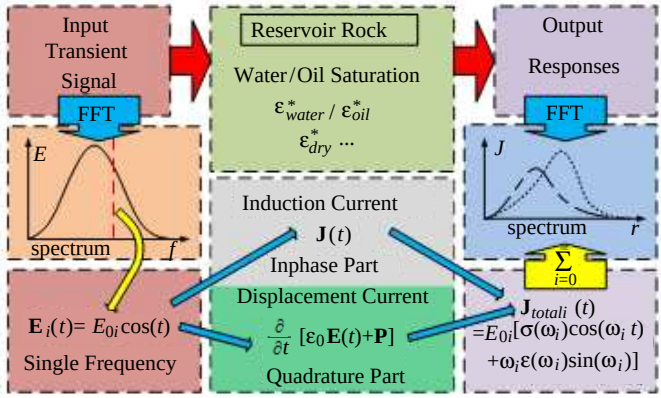

Figure 5. Block diagram illustrating linear system analysis of rock samples. This analysis method coincides with the physical mechanism. Through the linear system analysis of signals in rock samples, change discipline of response pulses can be obtained.

ring. Thus the basic idea of this approach conforms to the practical situation.

Three kinds of moist formation samples were used in this part: quartz sand soil, bentonite clay, and field sample from Kansas [29]. The model parameters used to describe the three different formations, and water Debye formulas are listed in Table 1.

Table 1. W_t is the maximum bound water fraction. σ_b, ε_{b0} and τ_b are conductivity, static dielectric constant and relaxation time of bound water, while σ_f, ε_{f0} and τ_f are free water's Debye parameters. ε_∞ and ε_d are dielectric constant of water in the high frequency limit and dry formation samples.

Formation Type	W_t	σ_t S/m	σ_f S/m	τ_b, S	τ_f, S	ε_{b0}	ε_{f0}	ε_∞	ε_d
Sand Soil			0.02		8.7×10^{-12}		80.7	4.9	3.08
Bentonite Clay	0.267	0.02	0.02	8.11×10^{-12}	8.68×10^{-12}	29.82	81.84	4.9	2.51
Field Sample	0.17	1.24	2.15	11.3×10^{-11}	8×10^{-12}	38.6	97.9	4.9	2.7

Fitting Debye formula parameters from experimental data into the GRMDM model, complex permittivity spectra of sand soil sample whose water saturation ranged from 10% to 70% were obtained as illustrated in Figure 6. As the water saturation increases, both the real and imaginary parts become bigger, and frequency dependence becomes more significant. Thus interfacial polarization and molecular polarization caused by the increasing water content dominate the electrical performance of the moist formation.

A broadband modulated Gaussian pulse with 500 MHz as the center frequency and a spectrum ranging to 1.5 GHz was chosen to be the input signal. The mathematical expression of the Gaussian is:

$$f(t) = -\cos\left(\pi \times 10^9\right) \exp\left[-\frac{4\pi(t - 8\times10^{-10})^2}{1\times10^{-18}}\right] \tag{16}$$

Center frequency and spectrum span could be changed according to the sensitive range of different formation texture. In the practical situation, transient pulse with frequency spectrum covering the sensitive frequency span could be an appropriate transmitting signal. Broadband pulses were used as excitation signals, which could provide an integrated spectrum of the complex permittivity. This method

could practically avoid wrong evaluation to the formation, when some frequency points were distorted.

The transient signal propagated through four moist sand formations with different water saturations as shown in Figure 6. After linear system analysis, response signals were determined to be two parts: amplitude and phase. Their amplitude spectrum could be obtained by subsequent inverse Fourier transform. Figure 7 illustrates how the input pulse shape changes with time and output pulse amplitudes of different responses in the frequency domain. The transient signal insures that the amplitude is large enough for

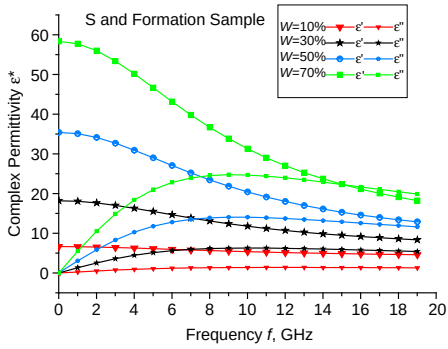

Figure 6. The complex permittivity of sand formation sample varies with water saturation. Real part and imaginary part of the complex permittivity are presented.

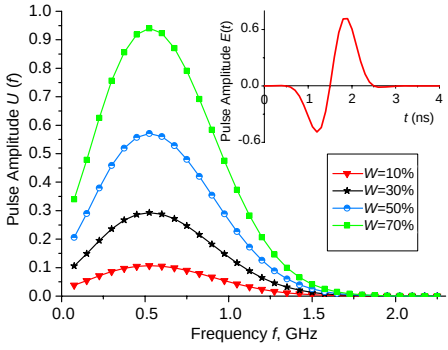

Figure 7. Top right graphic shows the shape of modulated Gaussian pulse, which is the transient signal in nanosecond order. The main graphic presents the response spectrum of four formations with saturation $W = 10\%; 30\%; 50\%; 70\%$.

detecting, because the pulse duration time is only several nanoseconds. There are obvious differences between the four response spectrums, which are influenced by water content. From the above data, the response amplitude spectrum is sensitive to the water saturation for the same rock texture. Evaluation of the formation water tendency can be achieved by analyzing the amplitude spectrum of the response signal.

For moist formation with different pore characteristics and physical structures, electrical performance of these samples generally varies, even if the water saturation is the same. The reason for this phenomenon is the existence of various types of rock water and different inherent structures for each kind of formation. For this purpose, in Figure 8 the complex permittivities of three kinds of formation with the same water saturation are presented. The rock samples discussed here are sand soil, bentonite clay and natural formation from Kansas reservoir, each of which has 70% pore water volumetrically.

Then we used modulated Gaussian pulse similar to that presented in Figure 7 as the excitation source for the three samples with different pore characteristics. In the same way, through linear system analysis and inverse Fourier transform, amplitude spectrums were achieved as indicated by Figure 9. There is recognizable diversity between these three frequency response curves, for three kinds of formations. Thus in the boundary between two formations whose structure is different

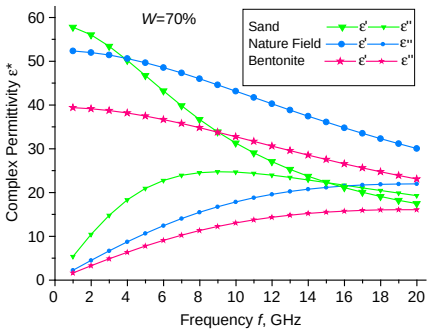

Figure 8. Sandy soils, bentonite clay, natural formation from Kansas have the same water saturation 70%. By GRMDM model, the real part and imaginary part of the three samples' complex permittivity are shown.

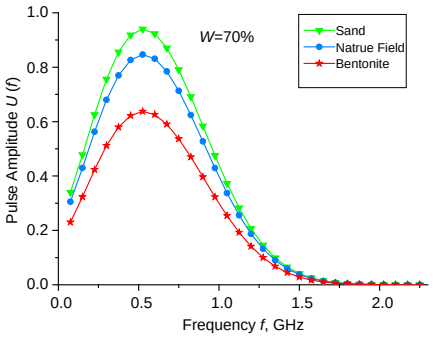

Figure 9. Three transient signal frequency responses are shown here. The three linear systems for signal testing are respectively sand soils, bentonite clay and natural formation from Kansas with water saturation of 70%.

with nearly the same water content, inherent texture change can be identified.

The Debye relaxation model can also be applied to describe complex permittivity of oil. Through fitting from practical measured data of oil [33], relaxation parameters for oil are given: $\tau_o = 0.6\,\text{ns}$, $\varepsilon_\infty = 1.1$, $\varepsilon_0 = 2.7$ [34]. Complex permittivity of sand formation with high oil saturation is presented in Figure 10 contrasting with that of water contained formation and dry sample. Relaxation frequency of oil is much lower than water's because of the microcosmic difference between hydrocarbon and water molecules. The dry sample's electric properties are independent of frequency, thus the imaginary part of its permittivity is approximately equal to zero.

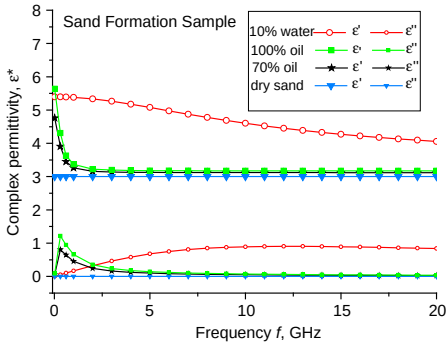

Figure 10. Complex permittivity of sand formation sample with saturation 70% and 100% are shown. Complex permittivity of dry sample and water contained sand formation's are references here.

The broadband Gaussian pulse and linear Fourier analysis processing in this part are as the above. The amplitude spectrum of response signals are presented in Figure 11. The response spectrum of the oil containing formation has a great amplitude difference compared to low water saturation formation. Furthermore, due to the disparate resonance peak, obvious shape changes are found in the response spectrum of the oil containing formation, especially in the frequency range below 1 GHz. The ratios of the response spectrum in oil and water saturated formations to that in dry formation demonstrate the responses differences in shape, while response in the water containing formation is almost proportional to the dry sample's response. These ratios are shown in the top right graph of Figure 11. In this way, in order to differentiate fluids contained in porous formation and to determine the saturation of fluid, both the amplitude ratio and spectrum shape can meet the requirement.

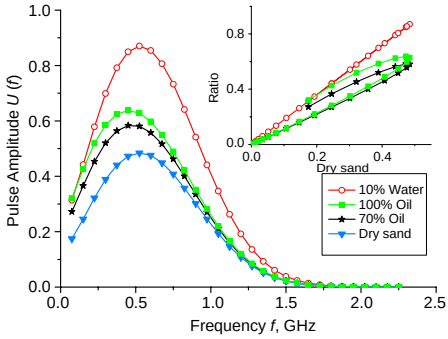

Figure 11. Four transient signal frequency responses are show. The four linear systems for signal testing are dry sand soil, sand soil with water saturation of 10%, and sand soil with oil saturation of 70% and 100%. Top right graph shows ratios of the response spectrum in oil and water saturated formations to that in the dry formation.

Linear system analysis is used as an analytic calculation method. Response signals obtained by this way are compared and validate the complex permittivity LWD system. Formations with the same texture and different saturations can be distinguished by the response signals, as well as formations with different textures and parallel saturation. The computed results demonstrate that the response spectrum image of the transient pulse provides satisfactory resolution and flexibility. Optimized results and sensitivity can be achieved, if the pulse type and frequency range are designed according to the actual situation. Thus analysis of the whole spectrum of response signals can achieve more integrated evaluation of formation saturation with smaller error.

5. CONCLUSION

An innovative complex permittivity logging tool excited by transient signal for LWD/MWD has been proposed in this paper. The near-bit current ring system is sensitive to the virgin zone close to borehole. The broadband spectrum of the transient pulse covers almost the whole frequency range in which a fluid containing formation's complex permittivity greatly depends on frequency. Analytic calculation accomplished by linear system Fourier analysis can achieve the response spectrums of a nanosecond pulse with a range from 20 MHz to 1.5 GHz. In this calculation both water and oil act as pore fluids in several kinds of natural formation samples, and different saturations are considered. Variation of fluid in formations causes obvious

changes in response amplitude and spectrum shape. Computed results prove that the tool presented here has many practical advantages compared with conventional complex permittivity logging tools, such as information integrity, anti-interference and reliability. In practical application, frequency range and pulse shape of the transient signal can be set according to the properties of the formation.

REFERENCES

1. Sun, X. Y., Z.-P. Nie, A. Li, and X. Luo, "Analysis and correction of borehole effect on the responses of multicomponent induction logging tools," *Progress In Electromagnetics Research*, Vol. 85, 211–226, 2008.
2. Hasar, U. C., "Permittivity determination of fresh cement-based materials by an open-ended waveguide probe using amplitude-only measurements," *Progress In Electromagnetics Research*, Vol. 97, 27–43, 2009.
3. Lee, K. Y., B.-K. Chung, Z. Abbas, K. Y. You, and E. M. Cheng, "Amplitude-only measurements of a dual open ended coaxial sensor system for determination of complex permittivity of materials," *Progress In Electromagnetics Research M*, Vol. 28, 27–39, 2013.
4. Adopley, J. A. K., D. G. Dudley, and R. Taherian, "Analytical models for determination of complex permittivity," *Progress In Electromagnetics Research*, Vol. 15, 109–139, 1997.
5. Tateiba, T. M. M., "Numerical analysis of scattered power from a layer of random medium containing many particles of high dielectric constant — Application to the detection of a water content of soil," *Progress In Electromagnetics Research*, Vol. 33, 199–218, 2001.
6. Von Hippel, A. R., Ed., *Dielectric Materials and Applications*, 36–40, MIT Press, Cambridge, 1954.
7. Boyarskii, D., V. V. Tikhonov, and N. Y. Komarova, "Model of dielectric constant of bound water in soil for applications of microwave remote sensing," *Progress In Electromagnetics Research*, Vol. 35, 251–269, 2002.
8. Bona, N., et al., "Electrical measurements in the 100 Hz to 10 GHz frequency range for efficient rock wettability determination," *SPE Journal*, Vol. 6, 80–88, 2001.
9. Garrouch, A. A. and M. M. Sharma, "The influence of clay content, salinity, stress, and wettability on the dielectric properties

of brine-saturated rocks: 10 Hz to 10 MHz," *Geophysics*, Vol. 59, 909–917, June 1994.

10. Wait, J., "Complex resistivity of the earth," *Progress In Electromagnetics Research*, Vol. 1, 1–173, 1989.
11. Meyer, W., et al., "Near-bit propagation resistivity for reservoir navigation," *SPE Annual Technical Conference and Exhibition*, 1994.
12. Zhang, Z., N. Yuan, and R. Liu, "1-D inversion of triaxial induction logging in layered anisotropic formation," *Progress In Electromagnetics Research B*, Vol. 44, 383–403, 2012.
13. Meyer, W. H., "Field measurements of resistivity dispersion using two frequency MWD propagation resistivity tools," *Petrophysics*, Vol. 41, 2000.
14. Hizem, M., et al., "Dielectric dispersion: A new wireline petrophysical measurement," *SPE Annual Technical Conference and Exhibition*, 2008.
15. Oh, J., E. J. Rothwell, D. P. Nyquist, and M. J. Havrilla, "Natural resonance representation of the transient field reflected by a conductor-backed lossy layer," *Journal of Electromagnetic Waves and Applications*, Vol. 17, No. 5, 673–694, 2003.
16. De Bibhas, R. and M. Nalson, "Ultrabroadband electromagnetic well logging a potential future technology," *Proc. 33rd Ann. Logging Symp. Trans., Soc. Professional Well Log Analysts*, 1992.
17. Rabinovich, M. B., et al., "Transient EM for geosteering and LWD/wireline formation evaluation," US Patent 8049507B2, 2011.
18. "DTEM with short spacing for deep, ahead of the drill bit measurements," WO Patent WO/2012/030, 768, 2012.
19. Epov, M., et al., "UWB electromagnetic borehole logging tool," *2010 IEEE International Geoscience and Remote Sensing Symposium (IGARSS)*, 3565–3567, 2010.
20. Epov, M., V. L. Mironov, and K. V. Muzalevskiy, "Method of measuring the range from the UWB borehole logging tool to the oil-water contact," *PIERS Online*, Vol. 7, No. 7, 689–692, 2011.
21. Epov, M. I., V. L. Mironov, K. V. Muzalevskiy, and I. N. Yeltsov, "UWB borehole logging tool to explore the electrical and structural properties of near-wellbore fluid-filled areas," *PIERS Online*, Vol. 7, No. 6, 559–562, 2011.
22. Ellis, D. V. and J. M. Singer, *Well Logging for Earth Scientists*, Springer, New York, 2007.
23. Olhoeft, G., "Low-frequency electrical properties," *Geophysics*,

Vol. 50, 2492–2503, 1985.

24. Malik, Q. M., B. R. P. da Rocha, and B. R. P. da Rocha, "High pressure electromagnetic fractal behaviour of sedimentary rocks," *Progress In Electromagnetics Research*, Vol. 19, 223–240, 1998.
25. Debye, P. J. W., *Polar Molecules,* 172, Dover, New York, 1929.
26. Seleznev, N., et al., "Dielectric mixing laws for fully and partially saturated carbonate rocks," *45th Annual Symposium*, Society of Petrophysicists & Well Log Analysts, Noordwijk, Netherlands, 2004.
27. Hallikainen, M. T., et al., "Microwave dielectric behavior of wet soil — Part 1: Empirical models and experimental observations," *IEEE Transactions on Geoscience and Remote Sensing*, 25–34, 1985.
28. Dobson, M. C., et al., "Microwave dielectric behavior of wet soil — Part II: Dielectric mixing models," *IEEE Transactions on Geoscience and Remote Sensing*, 35–46, 1985.
29. Mironov, V. L., et al., "Generalized refractive mixing dielectric model for moist soils," *IEEE Transactions on Geoscience and Remote Sensing,*, Vol. 42, 773–785, 2004.
30. Swiet, T. D., "An RF sensor for logging-while-drilling geophysical measurements," *Progress In Electromagnetics Research*, Vol. 17, 1–24, 1997.
31. Feliziani, M., et al., "FD2TD analysis of electromagnetic field propagation in multipole Debye media with and without convolution," *Progress In Electromagnetics Research B*, Vol. 42, 181–205, 2012.
32. Fuller, B. and S. Ward, "Linear system description of the electrical parameters of rocks," *IEEE Transactions on Geoscience Electronics*, Vol. 8, 7–18, 1970.
33. Saraev, D., et al., "Dielectric spectroscopy in studying mechanisms of structure-forming oils," *Electronic Scientific Journal, Oil and Gas Business*, http//www.ogbus.ru, 2005.
34. Epov, M., et al., "Nanosecond electromagnetic sounding of a fluid-saturated layered formation," *Russian Geology and Geophysics*, Vol. 48, 1054–1060, 2007.